DNA Repair

DOI: 10.1002/anie.200804268

Crystal Structure and Mechanism of a DNA (6-4) Photolyase**

Melanie J. Maul, Thomas R. M. Barends, Andreas F. Glas, Max J. Cryle, Tatiana Domratcheva, Sabine Schneider, Ilme Schlichting, and Thomas Carell**

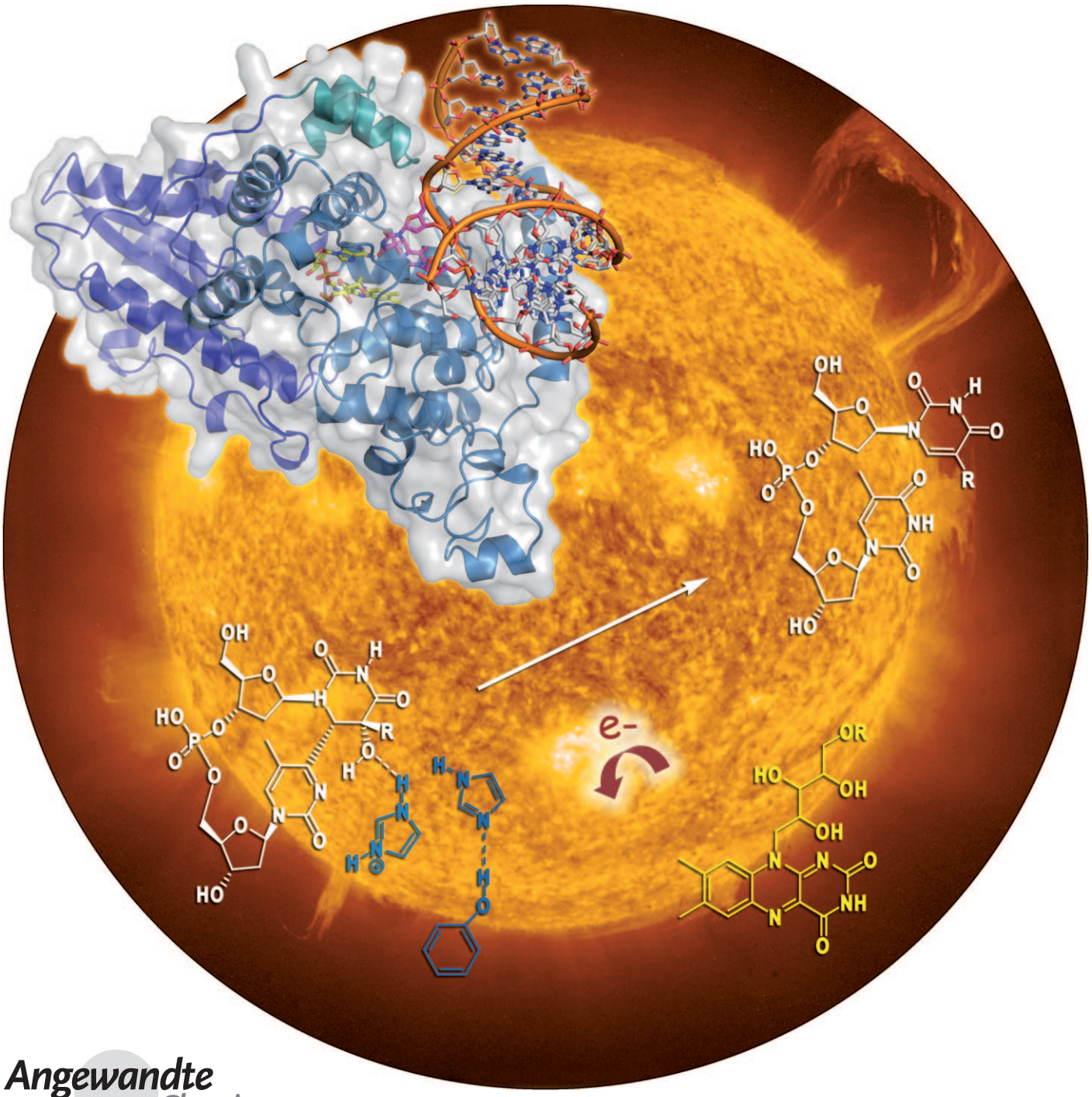

UV irradiation of cells gives rise to the formation of cyclobutane pyrimidine dimers (CPD) and so-called (6-4) DNA lesions (Scheme 1). Both lesions are major photoproducts formed in dipyrimidine sequences of double-stranded DNA.[1,2] Repair of these lesions is essential because of their high mutagenic potential. Particularly important in many organisms are the photolyase-mediated repair systems that are able to split CPD lesions and (6-4) lesions directly back into their corresponding monomers.[1,2] While formation and photolyase repair of CPD lesions is well studied, little is known about (6-4) lesions. In particular, the mechanism of repair of the (6-4) lesions by (6-4) DNA photolyases is a long-standing question. Currently it is believed that the enzyme rearranges the (6-4) lesion with the help of two conserved histidine residues in the active site to form an oxetane intermediate (Scheme 1), which is split after single-electron donation from a light-activated $FADH^-$.[3,4] We report here the first crystal structures of a (6-4) DNA photolyase enzyme. The structures show the enzyme in complex with a (6-4) lesion containing DNA before and after in situ repair. Based on the structural and biochemical data we propose a modified repair mechanism that lacks the strained oxetane intermediate.

For the structural analysis we irradiated DNA single strands containing only a single TT sequence flanked by G bases with UV light (254 nm) in a glove box. In such sequences the photochemical reactions take place at the dinucleotide TpT sequence.[5] The DNA strand containing the (6-4) lesion was isolated by HPLC (10% final yield; see Table S1 in the Supporting Information). We tested for the presence of a (6-4) lesion by full digestion of the irradiated DNA strands followed by HPLC-MS/MS analysis (Figures S1 and S2 in the Supporting Information) The DNA single strand containing the (6-4) lesion was hybridized with the corresponding counterstrand, and double strands with single nucleotide overhangs were used for crystallization. The strep-tagged (6-4) photolyase from *D. melanogaster* was cloned and overexpressed in *E. coli.* Pure protein was obtained by initially treating the cell lysate with Dnase I to digest bound DNA, followed by a *Strep-Tag II* column, and finally a heparin column.

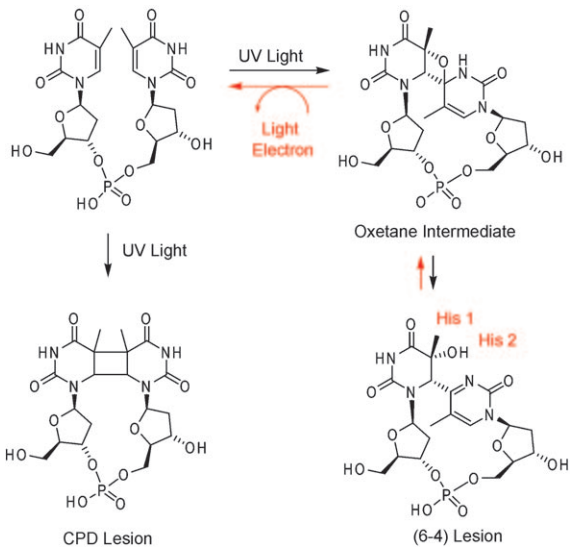

Scheme 1. Formation of CPD and (6-4) lesions and repair of the (6-4) lesion (in red) by first rearrangement of the (6-4) lesion into a putative oxetane intermediate with the help of two conserved histidine residues, followed by splitting as a result of light-induced electron transfer.

The oxidized (6-4) photolyase was cocrystallized in the dark with a 15-mer DNA duplex containing a central thymine–thymine (6-4) photolesion. The structure of the (6-4) photolyase was determined by the single-wavelength anomalous dispersion method using selenomethionine-labeled protein crystals (Table S2 in the Supporting Information). Two cocrystal structures were obtained: Firstly, the enzyme in complex with the T(6-4)T lesion in the active site determined to a resolution of 2.0 Å (Figure 1c) and secondly the (6-4) photolyase in complex with DNA containing the T(6-4)T lesion after dithionite reduction and irradiation of the crystals with white light (Figure 1d and Figure S3 in the Supporting Information). In the second case, the structure (at 2.7 Å resolution) shows a repaired TpT in the active site.

As anticipated, the (6-4) photolyase has the same overall fold as the previously reported CPD photolyases and cryptochromes, with an α/β domain and an FAD-binding helical domain (Figure 1a).[6–12] For lesion recognition, the (6-4) photolyase fully opens the DNA at the site of the lesion, and the (6-4) lesion flips out by almost 180° into the active site. Several protein residues (Figure 1b) stabilize the enormous bulge that is created by this event, including Arg421, which is a highly conserved residue in (6-4) photolyases. This residue protrudes into the duplex, stacking on top of the guanine base at the 3′-end of the (6-4) lesion and interacts with the phosphates of bases 9 (3.1 Å) and 10 (3.1 Å) of the damaged DNA strand. In a similar fashion, Lys431 and Ser424 interact with the phosphate oxygens of base 11 of the

[*] Dr. T. R. M. Barends,[+] Dr. M. J. Cryle, Dr. T. Domratcheva, Prof. Dr. I. Schlichting
Max Planck Institute for Medical Research
Department of Biomolecular Mechanisms
Jahnstrasse 29, 69120 Heidelberg (Germany)
E-mail: ilme.schlichting@mpimf-heidelberg.mpg.de
M. J. Maul,[+] A. F. Glas,[+] Dr. S. Schneider, Prof. Dr. T. Carell
Centre for Integrative Protein Science
Department of Chemistry and Biochemistry
Ludwig-Maximilians University Munich
Butenandtstrasse 5–13, 81377 Munich (Germany)
Fax: (+49) 892-1807-7756
E-mail: Thomas.carell@cup.uni-muenchen.de
[+] These authors contributed equally to this work.

[**] We thank J. C. Pieck and U. Hennecke for initial cloning and irradiation experiments. We are grateful to Ingrid Vetter for advice and support of the crystallographic software. We thank Armido Studer and Chrys Chatgilialoglu for very helpful discussions. Diffraction data were collected at the Swiss Light Source, beamline X10SA, Paul Scherrer Institute, Villigen, Switzerland. We thank the Dortmund–Heidelberg data collection team and the PXII staff for their support in setting up the beamline. This research was supported by the MPG, the Deutsche Forschungsgemeinschaft (SFB749 and SFB646), the Volkswagen Foundation, and the Excellence Cluster CIPS[M].

Supporting information for this article is available on the WWW under http://dx.doi.org/10.1002/anie.200804268.

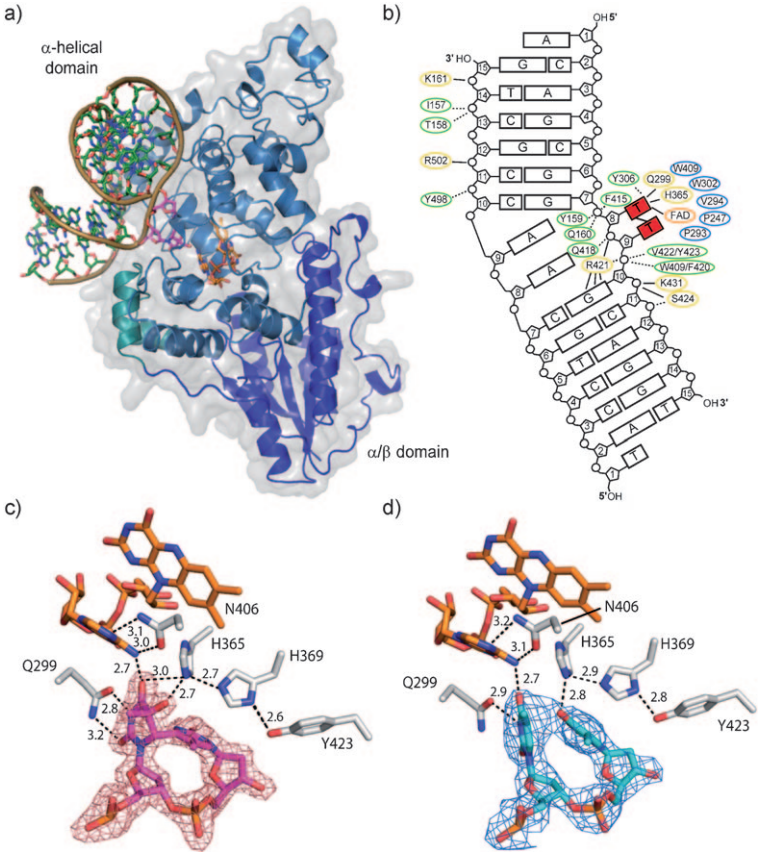

Figure 1. a) Overall structure of the (6-4) photolyase–DNA complex. b) Schematic diagram of the protein-DNA contacts. The flipped-out lesion is depicted in red, direct hydrogen-bond/electrostatic interactions are rendered in yellow, and water-mediated contacts in green and dashed lines. Residues forming the hydrophobic pocket around the pyrimidine substructure are shown in blue. c) Fo-*D*Fc-electron density map of the lesion after simulated annealing in CNS excluding the lesion both before ((c), lesion in pink) and after repair ((d), repaired DNA in cyan, contoured at the 3 σ level. Blue N, red O, orange carbon atoms of FAD, gray carbon atoms of amino acids in the active site.

damaged DNA strand (both 2.8 Å). In addition, Lys161 and Arg502 form salt bridges to the phosphate backbone of the undamaged strand downstream of the lesion, specifically to bases 14 and 12 (2.6 Å and 3.0 Å, respectively). The FAD is bound in a U-shaped conformation that is also observed in CPD photolyases and cryptochromes,[6–12] in which the adenine moiety folds back onto the ribityl chain protruding from the flavin ring system; it is held there by hydrogen bonds from its N1 and its NH_2 moiety to Asn406 (3.1 and 3.2 Å respectively). The lesion itself (Figure 1c) interacts with the protein by Watson–Crick-like hydrogen bonds between Gln299 and the pyrimidine N3 (2.8 Å) and O2 (3.2 Å), and a hydrogen bond between the pyrimidine C5 hydroxy group and His365 (2.8 Å), a residue that is fully conserved in (6-4) photolyases.[13] Apart from these interactions, the lesion is accommodated in a strikingly hydrophobic pocket lined by Trp302, Trp409, Pro247, Pro293, and Val294. The one water molecule observed in this pocket is hydrogen bonded to the C5 hydroxy group (2.9 Å) of the pyrimidine (Figure S4 in the Supporting Information).

In the structure containing the repaired TpT (Figure 1d), His365 stays in contact with the original C5 oxygen atom, which is, however, positioned at C4 of the 3′-thymine base after the transfer of the oxygen atom. Other than the transfer of this oxygen atom, only small structural changes in the active site are evident. Most critical is the observation that in the repaired complex Glu299 forms only one hydrogen bond to the TpT dinucleotide, which may facilitate the flipping back of the successfully repaired lesion. The crystal structures therefore suggest that the basic energy- and electron-transfer mechanisms utilized by the eukaryotic (6-4) photolyases are similar to those used by the bacterial class I CPD photolyases. After light absorption by $FADH^-$, electron transfer to the lesion occurs over a rather short distance of only 2.7 Å ($NH_{2,FADadenine}$—$O_{4,lesion}$), possibly with participation of the adenine moiety of FAD.

Next, we performed mutational studies to confirm the central hypothesis that the two conserved histidines His365 and His369, which are in close vicinity to the lesion, are essential for catalysis. Both these histidines and Tyr423, which interacts with His369, were mutated in turn. The mutant His365 to Asn365 was unable to repair the (6-4) lesion.[13] The second mutant His369 to Met369 shows low but clearly detectable residual repair activity (Figure S5 in the Supporting Information). The final mutation in the triad, Tyr423 to Phe423, also reduces the repair activity of the enzyme but to a lesser extent than the His369Met substitution, showing that the complete triad His365-His369-Tyr423 is important for catalysis. Crystal structures of the mutants confirm the structural integrity of their active sites.

The structural data of the (6-4) photolyase in complex with its substrate before and after in situ repair do not support the previously assumed oxetane-based mechanism depicted in Scheme 1. For this, one has to assume deprotonation of the C5-OH group by one of the conserved histidines, and a proton-catalyzed activation of the acylimine by the second. However, both histidines are positioned in such a way as to be unable to protonate the acylimine. In actual fact the acylimine is positioned in a largely hydrophobic environment (Figure 1b). The crystal structures show that the critical C5-OH group forms hydrogen bonds with water 276 (2.9 Å) and His365 (2.8 Å) (Figure 1c). His365, in turn, is in contact with His369 (2.8 Å), which itself establishes an interaction with the OH group of Tyr423 (2.6 Å). A recent ENDOR study by the Weber laboratory revealed that the histidine close to the ribityl chain of the FAD (H1′), which is His365 in our study, is likely protonated; this is not consistent with deprotonation of C5-OH.[14] We therefore believe that C5-OH is not deprotonated by the enzyme but converted into a better leaving group through protonation by His365. This, together with the inability to activate the acylimine are the main arguments against the oxetane intermediate (Scheme 1). The functional relevance of

our observations are confirmed by the fact that the crystals are enzymatically active such that the protein–DNA complex can react to yield the product upon irradiation of reduced crystals with white light. The direct transfer of the C5-OH group in the repair mechanism was confirmed by experiments performed in ^{18}O-labeled water, in which complete ^{16}O retention in the repaired DNA was observed.

Therefore, we propose a new mechanism in better agreement with the obtained structural insights. We currently believe (Scheme 2) that electron donation from the light-excited FAD occurs directly into the lesion, forming the radical anion **II**. After reduction, departure of the protonated C5-OH could give rise to intermediate **III**. The water molecule foemed could now attack the acylimine to form radical intermediate **IV**, possibly after activation by the histidines. Intermediate **IV** would rapidly fragment to give the repaired TpT, after reverse electron transfer to the FAD and loss of a proton.

To gain support for the formation of the postulated intermediate **III**, we directly compared repair of a T(6-4)T lesion (R = CH_3) and a U(6-4)T lesion (R = H) reasoning that the missing methyl group in the U(6-4)T lesion might reduce the stability of the radical intermediate **III** and slow down repair. This is indeed observed. DNA containing the U(6-4)T lesion is less efficiently repaired by a factor of 4 to 5 times (Figure S6 in the Supporting Information), a finding in support of the proposed mechanism depicted in Scheme 2.

In summary, we have described the first crystal structures of a (6-4) photolyase. The structural data show the enzyme in complex with DNA containing the (6-4) lesion before and after in situ repair. An oxetane intermediate was not detected in the unrepaired structure. In addition, we observe only small structural changes upon repair in the active site (Figure S3 in the Supporting Information). Given the position and the protonation state of the critical histidines, the $H_2{}^{18}O$ experiment revealing direct transfer of the C5-OH group, and the observation that repair of a U(6-4)T lesion is less efficient, the mechanism more likely follows a pathway similar to that depicted in Scheme 2 than the current postulate.

Experimental Section

D. melanogaster (6-4) photolyase was cloned into pDEST007,[15] expressed in *Escherichia coli* (Rosetta-gami pLysS (DE3); Novagen), and purified as an amino-terminally tagged *Strep-Tag II* fusion protein following treatment with DNAse I using a strep-tactin affinity column and with a heparin affinity column (Figure S7 in Supporting Information). The mutants were obtained by the QuickChange mutagenesis method (Stratagene). DNA containing the (6-4) lesion was obtained by irradiation of single-stranded DNA at 254 nm in a glove box under anaerobic conditions for 14 h. The strands were analyzed and purified by HPLC. The activity of the enzyme was determined by HPLC, using (6-4)-lesion-containing DNA as substrate (Figure S8 in Supporting Information). Formation of a short lived oxetane intermediate can not be ruled out. The enzyme/DNA mixture was irradiated for 1 h under white light; the reaction was stopped by heat denaturation of the photolyase. Co-crystals of the DNA-bound (6-4) photolyase were obtained by the hanging drop vapor diffusion method, using the enzyme (8.5 mg mL^{-1}) and DNA in a 1:1.1 molar ratio, mixed with equal volumes of reservoir solution (0.1 M Hepes, pH 7.0, 15–20 % (w/v) PEG 4000 or 0.1 M MIB buffer, pH 8.6, 20–25 % (w/v) PEG 1500). All crystallization studies were conducted under red-light conditions. The DNA repair reaction in the crystals was initiated by soaking the crystals in cryoprotecting solution containing reducing agent and then irradiating them with white light (see the Supporting Information for details). Data were collected at the Swiss Light Source, Villigen, Switzerland, and structure solution was carried out by means of single-wavelength anomalous dispersion, using selenomethionine-labeled protein. Initial phases were calculated with SHARP,[16,17] the models were constructed with ARP/wARP[18] and COOT,[19] and the structures were refined with REFMAC[20] and CNS.[21] The atomic coordinates and structure factors (PDB entries 3CVU and 3CVY)) have been deposited in the PDB, Collaboratory for Structural Bioinformatics, Rutgers University, New Brunswick, NJ (www.rcsb.org).

Received: August 29, 2008
Published online: October 27, 2008

Keywords: DNA damage · DNA repair · enzymes · photochemistry · structure elucidation

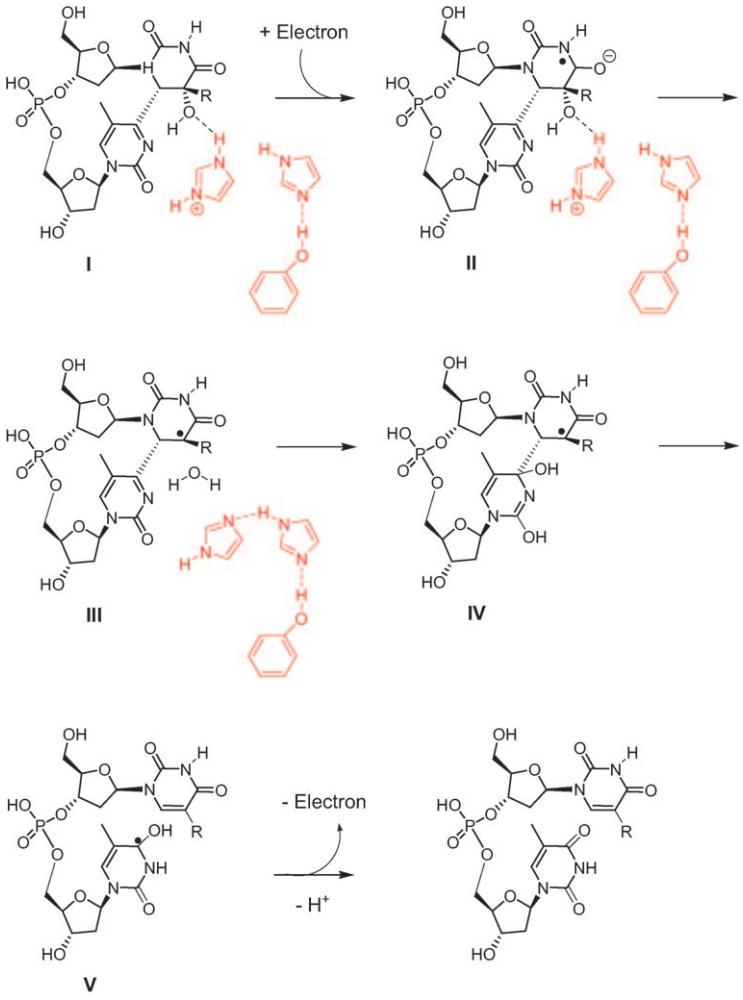

Scheme 2. Proposed repair mechanism for the light-induced, electron-transfer-based splitting of (6-4) lesions. T(6-4)T: R = CH_3, U(6-4)T: R = H.

[1] A. Sancar, *Chem. Rev.* **2003**, *103*, 2203 – 2237.
[2] R. P. Sinha, D.-P. Häder, *Photochem. Photobiol. Sci.* **2002**, *1*, 225 – 236.
[3] S. T. Kim, K. Malhotra, C. A. Smith, J. S. Taylor, A. Sancar, *J. Biol. Chem.* **1994**, *269*, 8535 – 8540.
[4] X. Zhao, J. Liu, D. S. Hsu, S. Zhao, J. S. Taylor, A. Sancar, *J. Biol. Chem.* **1997**, *272*, 32580 – 32590.
[5] L. M. Kundu, U. Linne, M. Marahiel, T. Carell, *Chem. Eur. J.* **2004**, *10*, 5697 – 5705.
[6] H. W. Park, S. T. Kim, A. Sancar, J. Deisenhofer, *Science* **1995**, *268*, 1866 – 1872.
[7] T. Tamada, K. Kitadokoro, Y. Higuchi, K. Inaka, A. Yasui, P. E. de Ruiter, A. P. Eker, K. Miki, *Nat. Struct. Biol.* **1997**, *4*, 887 – 891.
[8] R. Kort, H. Komori, S. Adachi, K. Miki, A. Eker, *Acta Crystallogr. Sect. D* **2004**, *60*, 1205 – 1213.
[9] A. Mees, T. Klar, P. Gnau, U. Hennecke, A. P. Eker, T. Carell, L. O. Essen, *Science* **2004**, *306*, 1789 – 1793.
[10] Y. Huang, R. Baxter, B. S. Smith, C. L. Partch, C. L. Colbert, J. Deisenhofer, *Proc. Natl. Acad. Sci. USA* **2006**, *103*, 17701 – 17706.
[11] T. Klar, R. Pokorny, J. Moldt, A. Batschauer, L. O. Essen, *J. Mol. Biol.* **2007**, *366*, 954 – 964.
[12] M. Fujihashi, N. Numoto, Y. Kobayashi, A. Mizushima, M. Tsujimura, A. Nakamura, Y. Kawarabayasi, K. Miki, *J. Mol. Biol.* **2007**, *365*, 903 – 910.
[13] K. Hitomi, H. Nakamura, S. T. Kim, T. Mizukoshi, T. Ishikawa, S. Iwai, T. Todo, *J. Biol. Chem.* **2001**, *276*, 10103 – 10109.
[14] E. Schleicher, K. Hitomi, C. W. Kay, E. D. Getzoff, T. Todo, S. Weber, *J. Biol. Chem.* **2007**, *282*, 4738 – 4747.
[15] M. Ober, H. Muller, C. Pieck, J. Gierlich, T. Carell, *J. Am. Chem. Soc.* **2005**, *127*, 18143 – 18149.
[16] C. Vonrhein, E. Blanc, P. Roversi, G. Bricogne, *Methods Mol. Biol.* **2007**, *364*, 215 – 230.
[17] E. de La Fortelle, G. Bricogne, *Methods Enzymol.* **1997**, *276*, 472 – 494.
[18] A. Perrakis, R. Morris, V. S. Lamzin, *Nat. Struct. Biol.* **1999**, *6*, 458 – 463.
[19] P. Emsley, K. Cowtan, *Acta Crystallogr. Sect. D* **2004**, *60*, 2126 – 2132.
[20] G. N. Murshudov, A. A. Vagin, E. J. Dodson, *Acta Crystallogr. Sect. D* **1997**, *53*, 240 – 255.
[21] A. T. Brünger, P. D. Adams, G. M. Clore, W. L. DeLano, P. Gros, R. W. Grosse-Kunstleve, J. S. Jiang, J. Kuszewski, M. Nilges, N. S. Pannu, R. J. Read, L. M. Rice, T. Simonson, G. L. Warren, *Acta Crystallogr. Sect. D* **1998**, *54*, 905 – 921.